Shallow water remote sensing using Hyperspectral imagery and bathymetric LiDAR

Zhigang Pan, Craig Glennie,
Juan Carlos Fernandez-Diaz, Ramesh Shrestha

Geosensing System Engineering and Science
National Center for Airborne Laser Mapping
Cullen College of Engineering
University of Houston

Case 1: Study Areas and Datasets

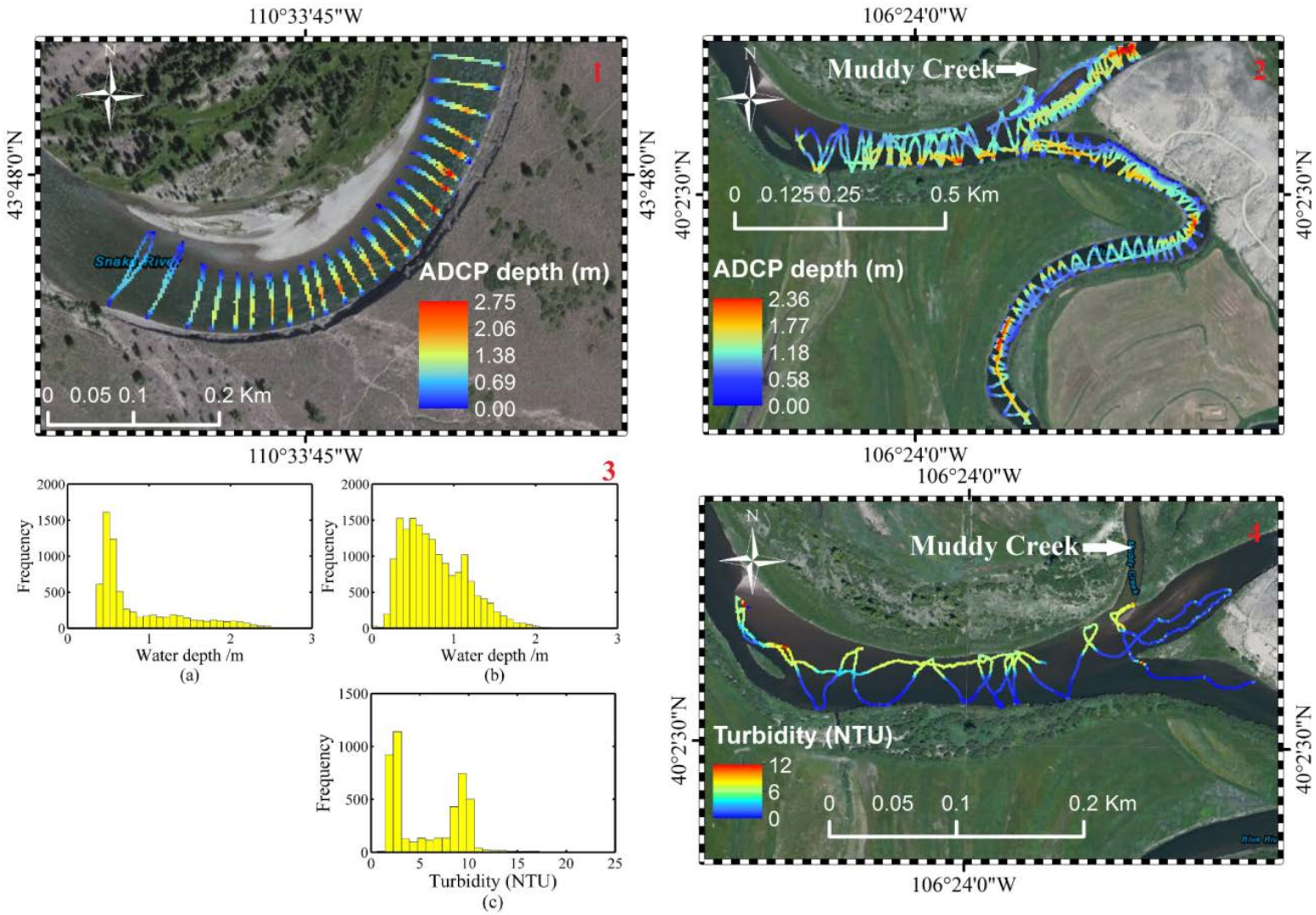

Study Areas and Datasets

	Snake River		Blue/Colorado River	
	LiDAR(green,NIR)	Optical	LiDAR(green,NIR)	Optical
Pulse width (ns)	8.3,12	N/A	8.3,12	N/A
Field of view (°)	40,46	40	40,46	40
Beam divergence (mrad)	1,0.8	N/A	1,0.8	N/A
Pulse rate (kHz)	33,100	N/A	33,100	N/A
Flight height (m)	512,585	585	587,2620	2620
Point density (pts/m^2)	4.2,6.3	N/A	4.0,2.5	N/A
Number of spectral bands	N/A	22	N/A	64
Pixel size (m)	N/A	0.6	N/A	1.2

Radiative transfer-Simplified Model

Simplified model given by Philpot (1989):

$$R(0^-) = R_\infty(1 - \exp(-g \cdot d)) + A_d \exp(-g \cdot d)$$

$$= R_\infty + (A_d - R_\infty)\exp(-g \cdot d)$$

Water column reflectance | Benthic contrast | Effective attenuation | Depth

- Linear method (Principal Component Analysis, PCA);
- Band ratio method.

Radiative Transfer - Airborne LiDAR Bathymetry

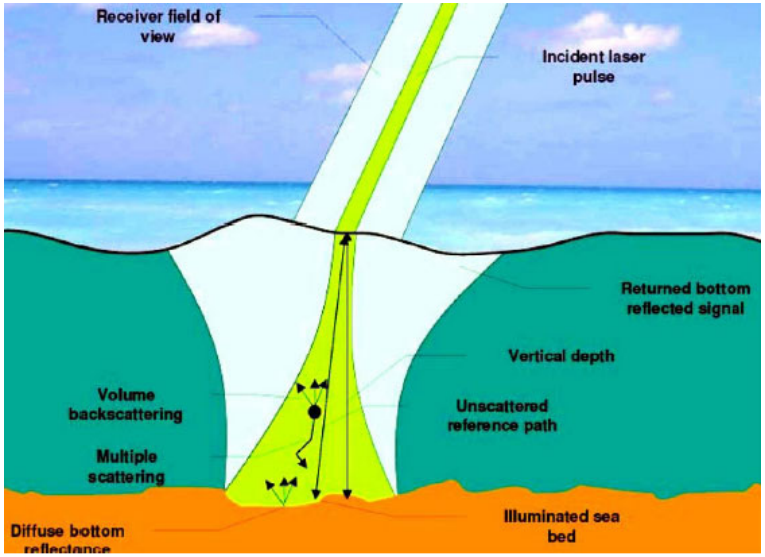

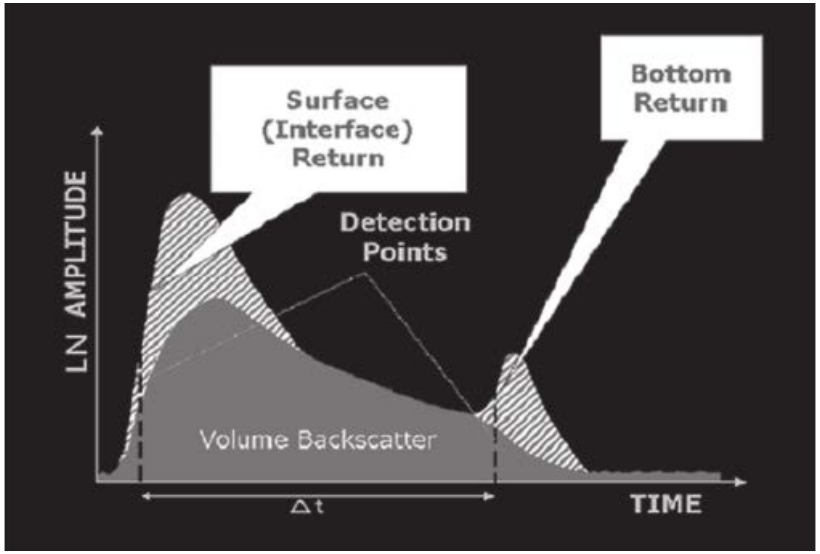

Figure 1 and 2 are courtesy of Guenther, (2007)

$$S_t(t) = S_s(t) + S_c(t) + S_b(t)$$

- Complex radiative transfer models;
- Many factors are involved;
- Difficulties to predict the performance of a specific bathymetric LiDAR

Hyperspectral Imagery vs. Bathymetric LiDAR

Hyperspectral imagery	Bathymetric LiDAR
Pros: 1. Fine spectral information; benefits classification, bathymetry retrieval, improved bathymetry, etc. 2. Flexibility of deployment.	Pros: 1. Direct measurements; 2. Relatively consistent accuracy; 3. High flexibility of deployment; 4. Better penetration due to the higher energy of laser pulse used.
Cons: 1. Field data; 2. Recorded in digital numbers; 3. Optimal collection time near local noon; 4. Complex radiative transfer process; 5. Tradeoff between spatial and spectral resolution.	Cons: 1. Monochromatic observation; 2. Turbidity affects the measurements significantly; 3. Limited algorithms.

From full waveform to orthowaveforms-Voxelization

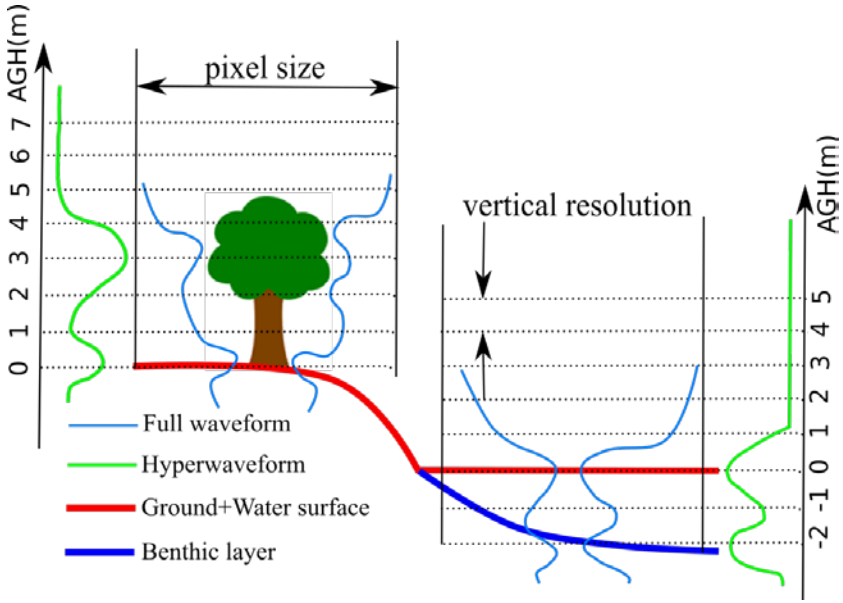

- Georeference of the recorded full waveform;
- Digital Terrain Model (DTM, generated from LiDAR) was applied;
- Generate orthowaveforms with voxelization.

Park, J. Y.; Ramnath, V.; Tuell, G. Using lidar waveforms to detect environmental hazards through visualization of the water column. In *OCEANS 2014 - TAIPEI*; IEEE, 2014; pp. 1–5.

Hyperspectral vs. Orthowaveforms-Snake River

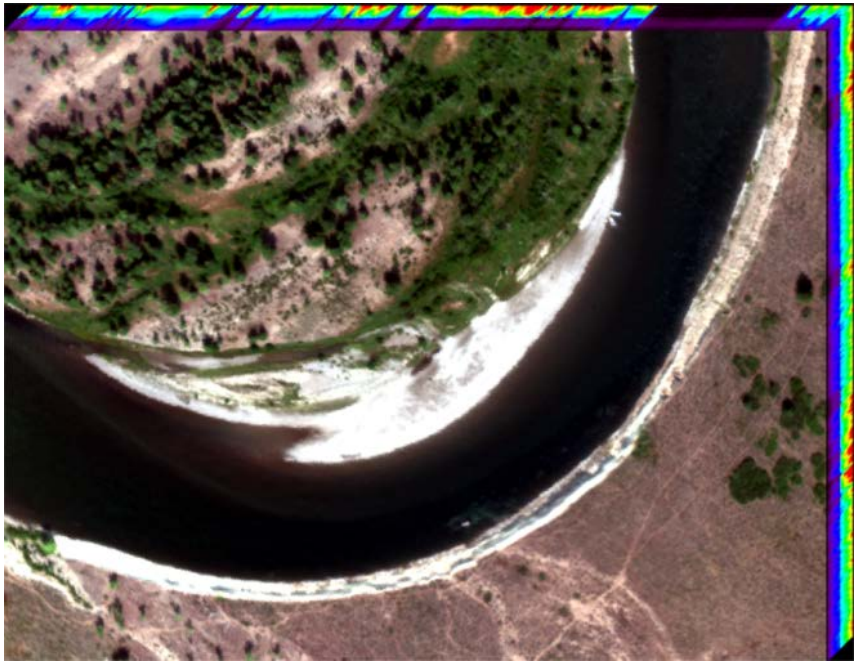

Hyperspectral

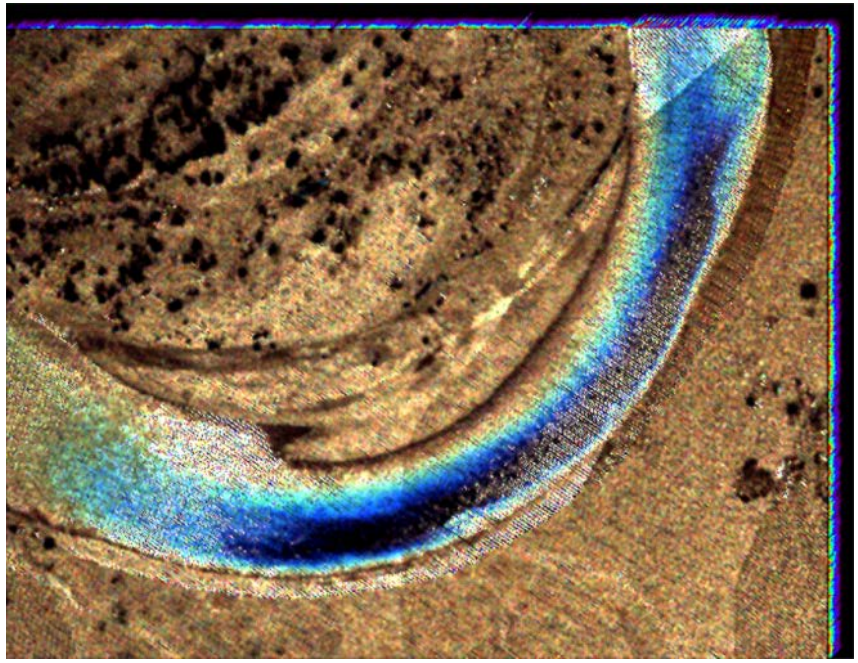

Orthowaveform

Orthowaveform imagery has 0.6 m for the pixel size and 0.2 m for the vertical resolution

Hyperspectral vs. Orthowaveforms-Blue/Colorado River

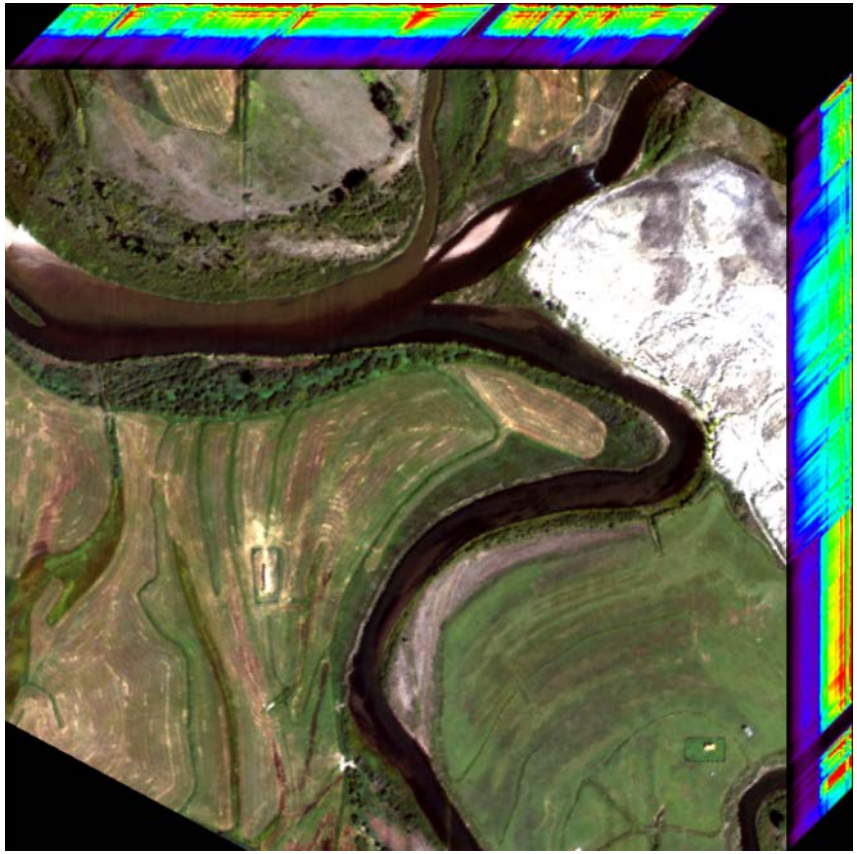

Hyperspectral

Orthowaveform

Orthowaveform imagery has 1.2 m for the pixel size and 0.2 m for the vertical resolution

Support Vector Regression (SVR)

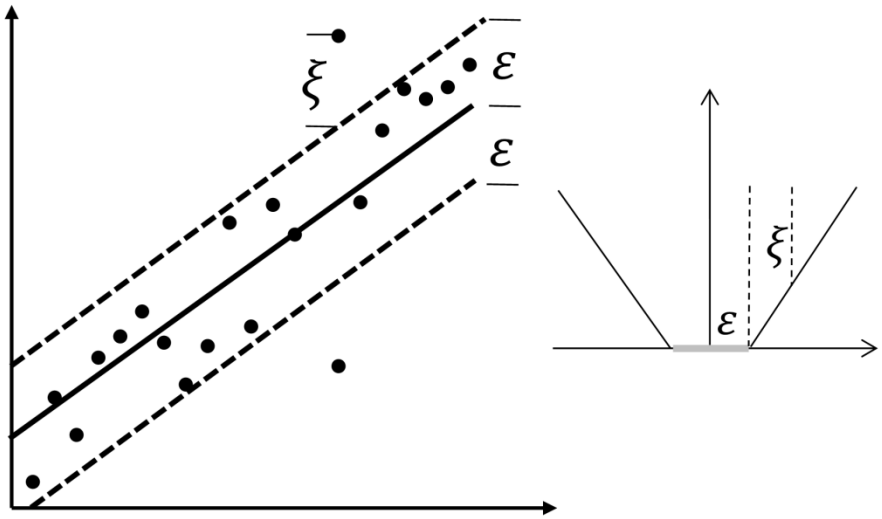

$$\text{Min:} \frac{1}{2}\|\mathbf{w}\|^2 + C\sum_{i=1}^{n}(\xi_i + \xi_i^*)$$

$$\text{Subject to} \begin{cases} y_i - f(x_i) \le \varepsilon + \xi_i^*; \\ f(x_i) - y_i \le \varepsilon + \xi_i; \\ \xi_i, \xi_i^* \ge 0, i = 1, \cdots, n \end{cases}$$

- SVR is an advanced non-parametric regression algorithm (no explicit model);
- Kernel function is used for reprojection;
- Cross-validation is used to search for the optimum SVR coefficients (data dependent).

Chang, C.-C.; Lin, C.-J. LIBSVM: a library for support vector machines. *ACM Trans. Intell. Syst. Technol.* **2011**, *2*, 27.

Bathymetry retrieval-Snake River

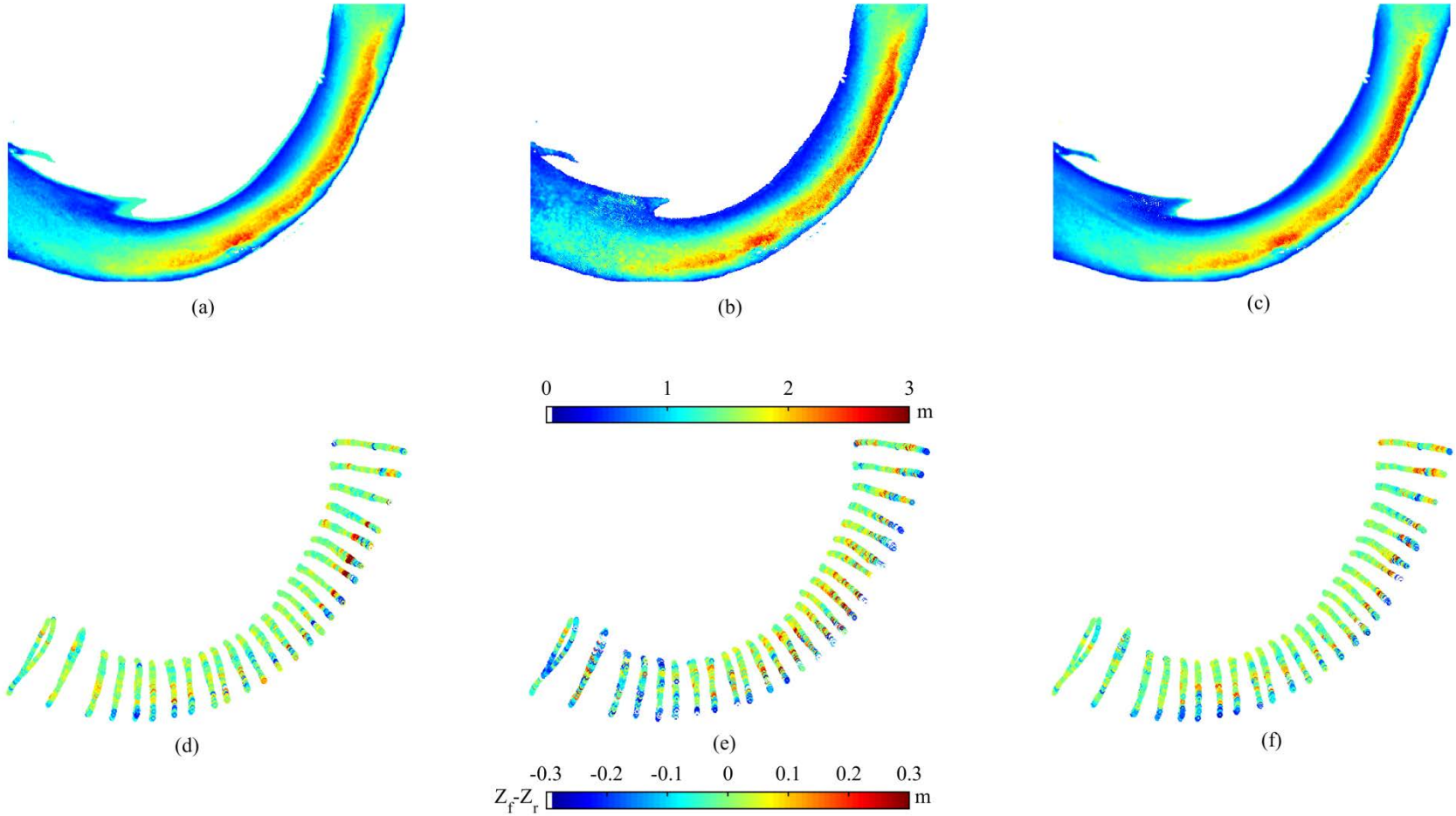

Hyperspectral | Orthowaveform | Fusion

Bathymetry retrieval-Snake River

	Hyperspectral		Orthowaveforms		Fusion	
κ	RMSE(m)	R^2	RMSE(m)	R^2	RMSE(m)	R^2
100	0.16(0.07)	0.91(0.08)	0.21(0.02)	0.86(0.03)	0.13(0.01)	0.94(0.01)
200	0.16(0.07)	0.91(0.07)	0.18(0.01)	0.89(0.01)	0.12(0.01)	0.96(0.01)
300	0.12(0.03)	0.95(0.02)	0.18(0.01)	0.90(0.01)	0.11(0.01)	0.96(0.01)
400	0.12(0.02)	0.95(0.02)	0.17(0.01)	0.90(0.01)	0.11(0.01)	0.96(0.00)
500	0.11(0.03)	0.96(0.03)	0.17(0.01)	0.91(0.01)	0.10(0.01)	0.96(0.01)

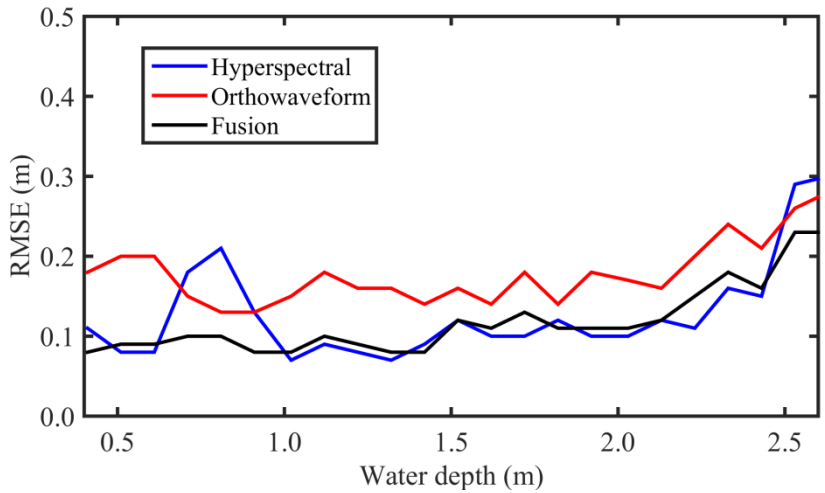

Bathymetry retrieval-Blue/Colorado River

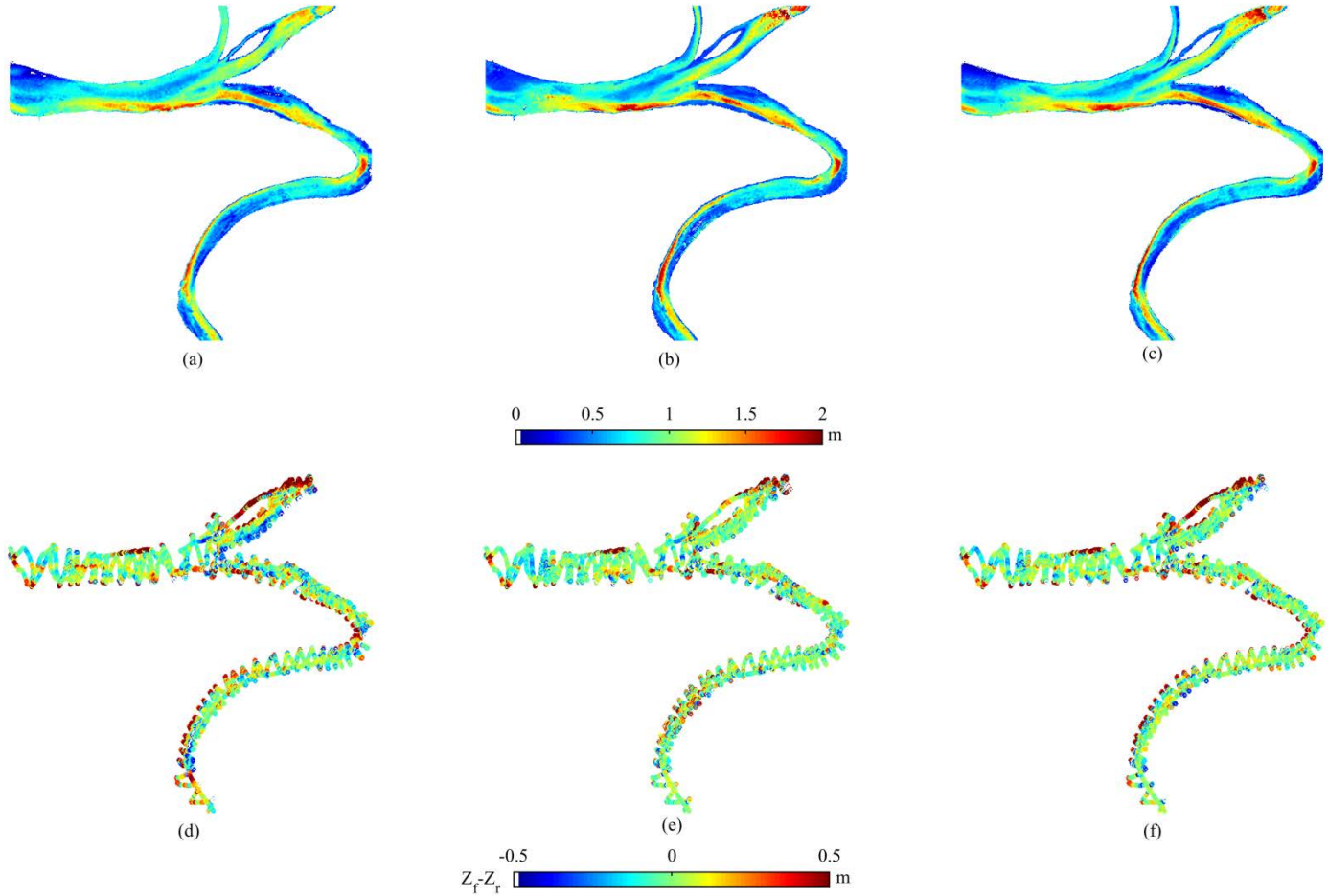

Hyperspectral Hyperwaveform Fusion

Bathymetry retrieval-Blue/Colorado River

	Hyperspectral		Orthowaveforms		Fusion	
κ	RMSE(m)	R^2	RMSE(m)	R^2	RMSE(m)	R^2
100	0.33(0.03)	0.40(0.09)	0.25(0.03)	0.60(0.07)	0.25(0.02)	0.60(0.04)
200	0.28(0.02)	0.50(0.05)	0.23(0.03)	0.66(0.06)	0.23(0.02)	0.65(0.04)
300	0.27(0.02)	0.52(0.05)	0.21(0.01)	0.70(0.03)	0.22(0.01)	0.69(0.03)
400	0.26(0.01)	0.55(0.03)	0.21(0.01)	0.71(0.02)	0.21(0.01)	0.70(0.03)
500	0.26(0.01)	0.55(0.04)	0.21(0.02)	0.70(0.04)	0.21(0.01)	0.71(0.03)

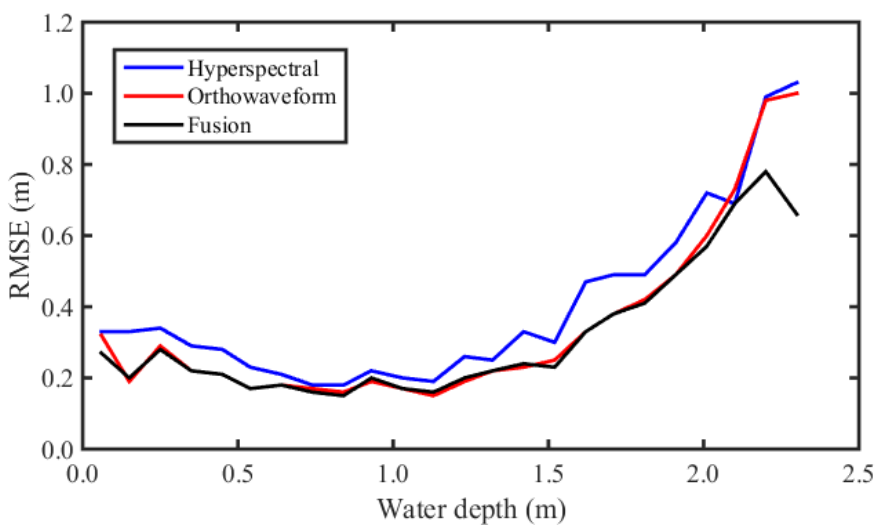

Water turbidity retrieval-Blue/Colorado River

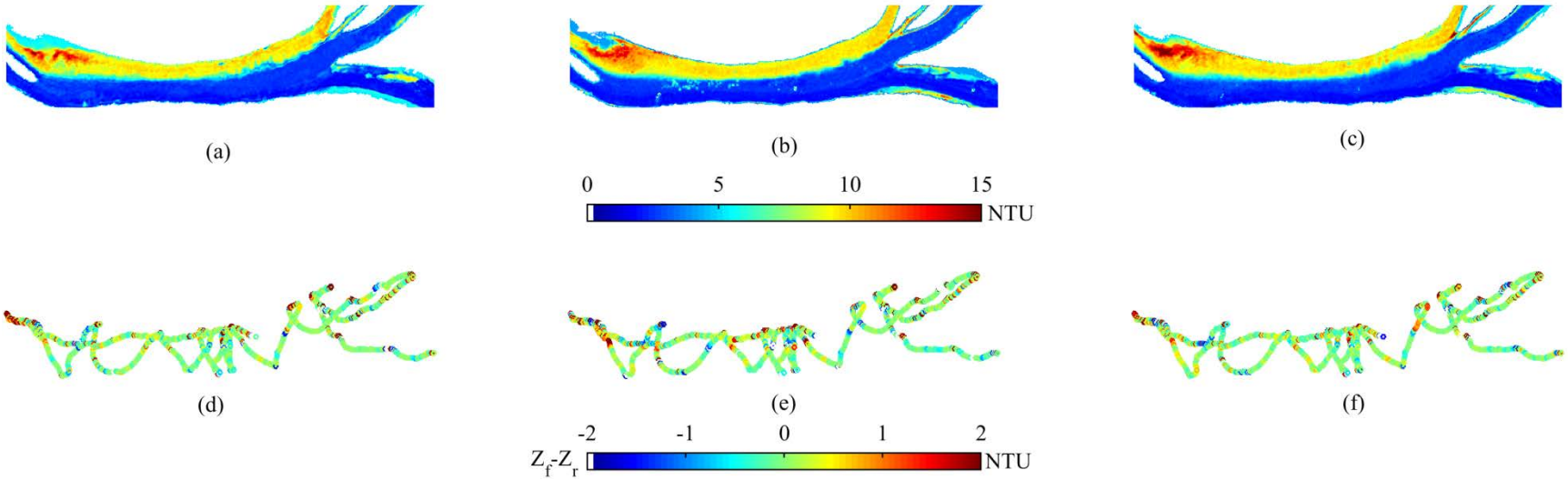

Water turbidity retrieval-Blue/Colorado River

	Hyperspectral		Orthowaveforms		Fusion	
κ	RMSE(NTU)	R^2	RMSE(NTU)	R^2	RMSE(NTU)	R^2
100	1.59(0.22)	0.81(0.04)	1.52(0.12)	0.82(0.02)	1.45(0.13)	0.84(0.02)
200	1.42(0.13)	0.84(0.03)	1.50(0.10)	0.82(0.02)	1.37(0.11)	0.85(0.02)
300	1.31(0.07)	0.86(0.01)	1.41(0.09)	0.84(0.02)	1.23(0.05)	0.88(0.01)
400	1.25(0.08)	0.87(0.02)	1.38(0.06)	0.84(0.01)	1.21(0.05)	0.88(0.01)
500	1.20(0.08)	0.88(0.01)	1.32(0.08)	0.86(0.02)	1.16(0.08)	0.89(0.01)

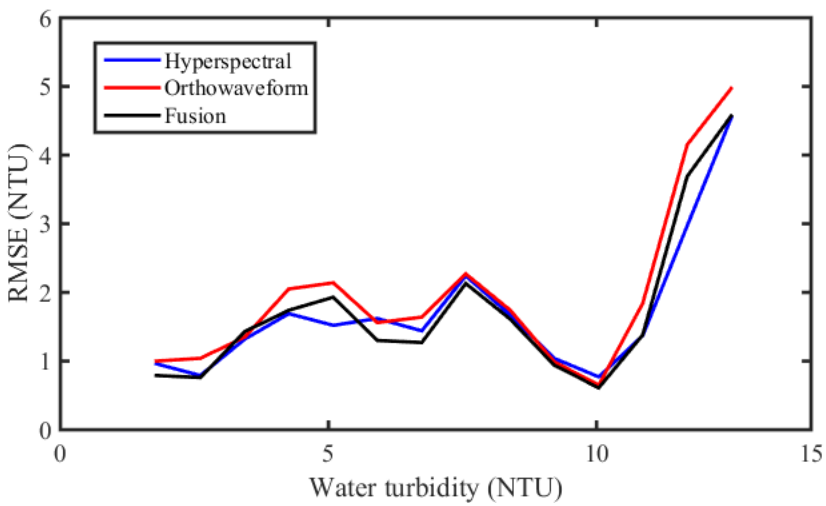

Orthowaveforms vs. full waveform bathymetry

	Snake River		Blue/Colorado River	
	Full waveform	Orthowaveform	Full waveform	Orthowaveform
Mean (Z_f-Z_r, m)	-0.13	-0.04	-0.16	-0.01
Std (Z_f-Z_r, m)	0.13	0.16	0.27	0.20
Slope	1.08	0.93	0.85	0.84
Intercept	0.05	0.12	0.28	0.15
R^2	0.92	0.92	0.57	0.73

*Z_f is the field measurement, Z_r is LiDAR derived water depth, Std: standard deviation

Orthowaveform outperforms full waveform decomposition in more turbid water (Blue/Colorado River)

Problems

- SVR is a supervised method; training data is required!
- Only the turbidity is retrieved; other water column characteristics parameters are expected;
- More fusion strategies need to be investigated.

Case 2: Study area

- The East Pass is located in Destin, Florida. Outlet for Choctawhatchee Bay
- 423 ADCP depth samples cocollected with the airborne datasets

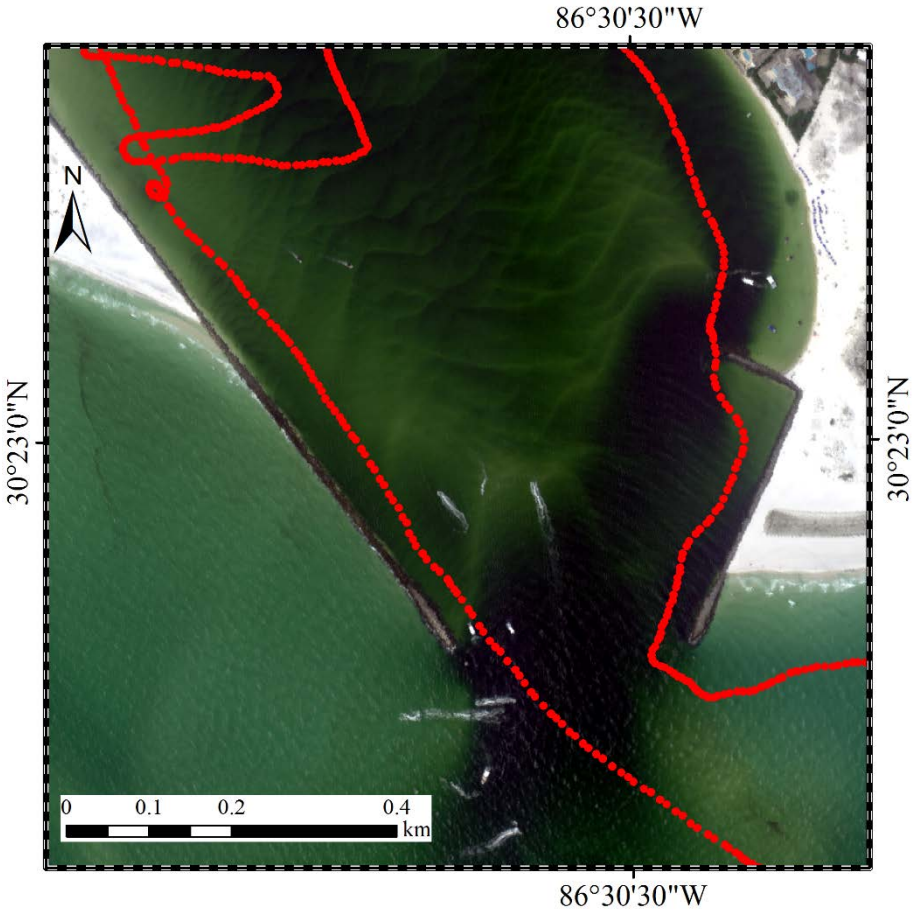

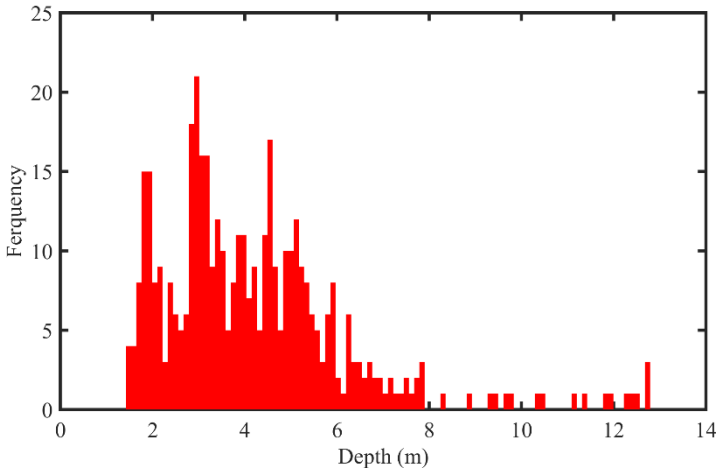

Data acquisition

Principal acquisition parameters

	LiDAR (532, 1064, 1550, nm)	Optical
Pulse width (ns)	2.5, 2.5, 2.5	N/A
Field of view (°)	30, 30, 30	N/A
Beam divergence (mrad)	0.7, 0.35, 0.35	N/A
Pulse rate (kHz)	100,100,100	N/A
Flight height (m)	300 to 500	2200
Point density (pts/m^2)	4.0, 4.0, 4.0	N/A
Number of bands	N/A	48
Pixel size (m)	N/A	1

Field white sand spectra

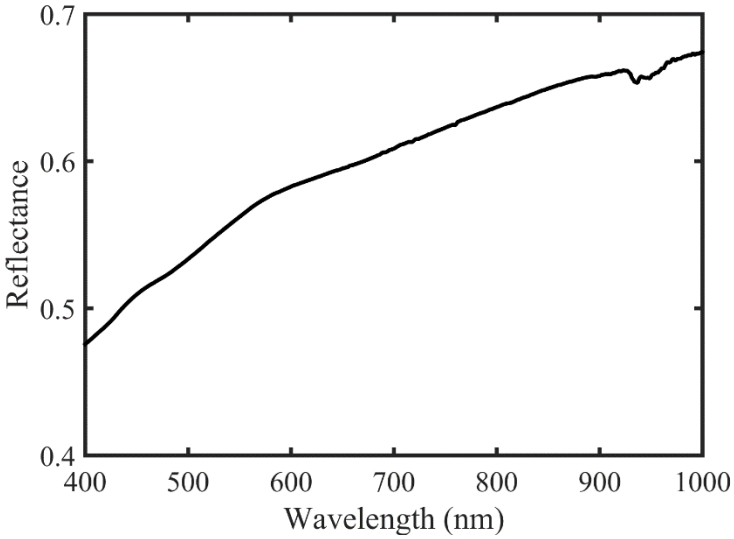

White sand prevails at the study area and the field measured white sand spectra is used in the seminanalytical model

Radiative transfer-Two alternatives

Mobley's HydroLight numerical simulation package.

- Use Monte Carlo techniques and probability theory to simulate the radiative transfer process in water body;
- This model is simple and very general;
- Forward Model and not invertible;
- Commercial package.

Lee's Semianalytical model

- An "approximation" to HydroLight software package;
- Combine the analytical and empirical models;
- Invertible!
- Widely implemented.

Radiative transfer-Subsurface reflectance

Subsurface remote sensing reflectance:

$$r(\lambda) = r_{\infty}(\lambda)\left(1 - e^{-\left(k_d(\lambda)+k_u^c(\lambda)\right)d}\right) + \frac{R_{0,B}(\lambda)}{\pi} e^{-\left(k_d(\lambda)+k_u^b(\lambda)\right)d}$$

- $r(\lambda)$ is the subsurface remote sensing reflectance;
- $r_{\infty}(\lambda)$ is the deep water remote sensing reflectance;
- $k_d(\lambda)$ is the downward attenuation coefficient;
- $k_u^c(\lambda)$ is the upward water column attenuation coefficient;
- $k_u^b(\lambda)$ is the upward benthic attenuation coefficient;
- $R_{0,B}(\lambda)$ is the normalized benthic albedo;
- d is the water optical depth.

Radiative transfer-Water attenuation coefficients

$$k_d(\lambda) = \frac{a(\lambda) + b_b(\lambda)}{\cos(\theta_s)}$$

$$k_u^c(\lambda) = \frac{1}{\cos(\theta_v)}(1.03(a(\lambda) + b_b(\lambda)))(1 + 2.4\frac{b_b(\lambda)}{a(\lambda) + b_b(\lambda)})^{0.5}$$

$$k_u^b(\lambda) = \frac{1}{\cos(\theta_v)}(1.04(a(\lambda) + b_b(\lambda)))(1 + 5.4\frac{b_b(\lambda)}{a(\lambda) + b_b(\lambda)})^{0.5}$$

$$r_\infty(\lambda) = (0.084 + 0.17\frac{b_b(\lambda)}{a(\lambda) + b_b(\lambda)})\frac{b_b(\lambda)}{a(\lambda) + b_b(\lambda)}$$

- $a(\lambda)$ is the water absorption coefficient;
- $b_b(\lambda)$ is the water backscattering coefficient;
- θ_s is the solar zenith angle;
- θ_v is the view angle.

Radiative transfer-IOPs

$$a(\lambda) = a_w(\lambda) + \left(a_0(\lambda) + a_1(\lambda)\right)\ln\left(0.06{C_{CHL}}^{0.65}\right)0.06{C_{CHL}}^{0.65}$$

$$+C_{CDOM}e^{-S_{CDOM}(\lambda-\lambda_0)} + C_{NAP}a^*_{NAP}(\lambda_0)e^{-S_{NAP}(\lambda-\lambda_0)}$$

$$b_b(\lambda) = b_{b,w}(\lambda)C_{CHL}b^*_{b,CHL}(\lambda_1)\left(\frac{\lambda_1}{\lambda}\right)^{Y_{CHL}} + C_{NAP}b^*_{b,NAP}(\lambda_1)\left(\frac{\lambda_1}{\lambda}\right)^{Y_{NAP}}$$

- $a_w(\lambda), b_{b,w}(\lambda)$ are the IOPs (Inherence Optical Properties, absorption and backscattering coefficients respectively) for pure sea water;
- $a_0(\lambda), a_1(\lambda)$ are the wavelength dependent model coefficients;
- $a^*_{NAP}(\lambda_0)$ is the NAP absorption coefficient at the reference wavelength
- $b^*_{b,CHL}(\lambda_1), b^*_{b,NAP}(\lambda_1)$ are the backscattering coefficients at the reference wavelength for CHL and NAP;
- $C_{CHL}, \mathrm{C_{CDOM}}, \mathrm{C_{NAP}}$ are the water constituent concentrations;
- S_{CDOM}, S_{NAP} are the spectral slope constants for CDOM and NAP;
- λ_0, λ_1 are the reference wavelengths;
- Y_{CHL}, Y_{NAP} are the power law exponents for CHL and NAP.

Radiative transfer-Water leaving reflectance

$$R(\lambda) = \frac{0.5r(\lambda)}{1 - 1.5r(\lambda)}$$

$R(\lambda)$ is the water leaving reflectance, that has taken account of the internal water refraction at the water-air interface.

The water leaving reflectance can be described as a function of the chlorophyll, color dissolved organic matter, non-algal particles and water depth:

$$R(\lambda) = f(C_{CHL}, C_{CDOM}, C_{NAP}, d)$$

LiDAR bathymetry and ADCP depths

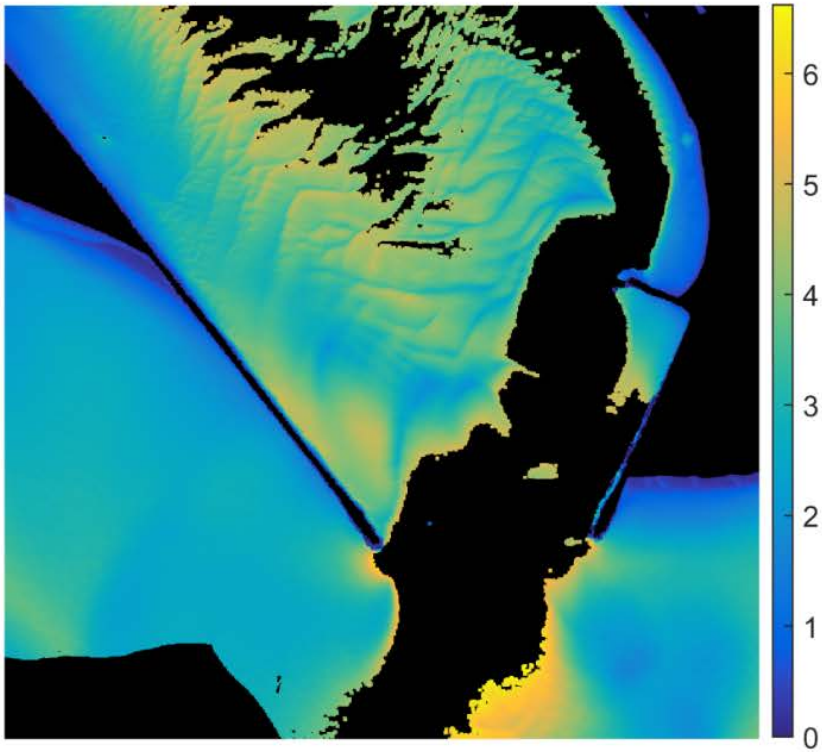

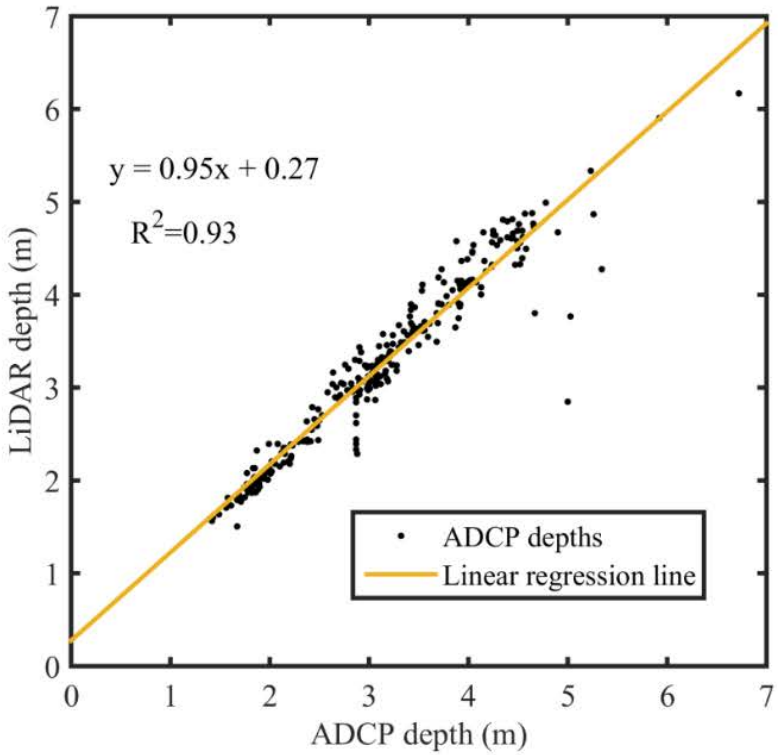

- LiDAR measures water depth up to ~7 m
- ADCP water depths match LiDAR depths well with R^2 of 0.93

Nonlinear Least Square method (nLSQ)

The objective function is:

$$\arg\min \sum_{i=0}^{n} \frac{\sqrt{(\mathbf{R}-\mathbf{r})^2}}{\mathbf{R}}$$

An example of the nLSQ modeled result and the original spectra:

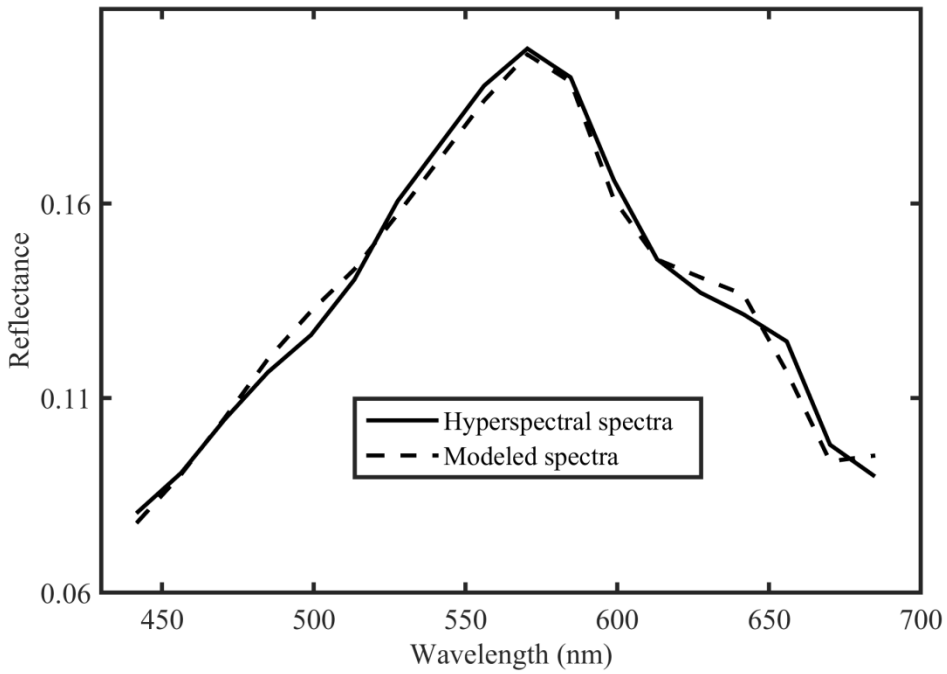

nLSQ, ranges and initial values

The range and the initial value for each parameter is determined through the unbounded nLSQ method due to the lack of the field measurements.

Parameters	Range	Initial value
C_{CHL} $(\mu g \cdot L^{-1})$	0.0-2.2	0.07
$C_{CDOM}(m^{-1})$	0.0-1.0	0.5
$C_{NAP}(mg \cdot L^{-1})$	0-15	10
$d(m)$	0-7	2

*The range and the initial value are critical for nLSQ because of it searches for the local minima.

Artificial spectra

Artificial spectra is produced using the forward semianalytical model fed with artificial environmental parameters and water depths;

The example spectra generated with fixed water column characteristics and the varying water depths:

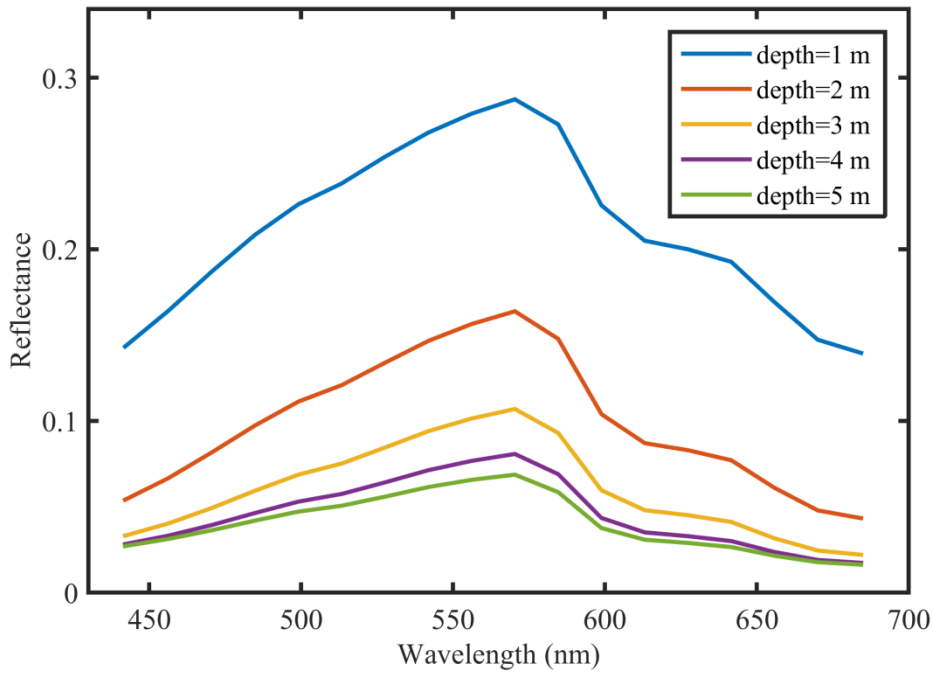

SVR-Sampling strategy

$$R(\lambda) = f(C_{CHL}, C_{CDOM}, C_{NAP}, d)$$

Two sampling strategies are available:

Exhaustive sampling: make fine resolution samples for every parameter and make combinations ($N_{samples} = N_{CHL} * N_{CDOM} * N_{NAP} * N_d$, here N is the number of samples).

Pros: Accurate
Cons: Computationally expensive!

Random sampling: randomly select combinations within the specified range.

Pros: Light computation
Cons: Less accurate

A sensitivity analysis was performed to investigate the influence of the number of samples for calibration.

mSVR, sensitivity analysis

Sensitivity analysis: increase the sample size from 100 to 1000 and each experiment was repeated for 10 times, the mean and the standard deviation of RMSE are used to determine the optimal calibration sample size.

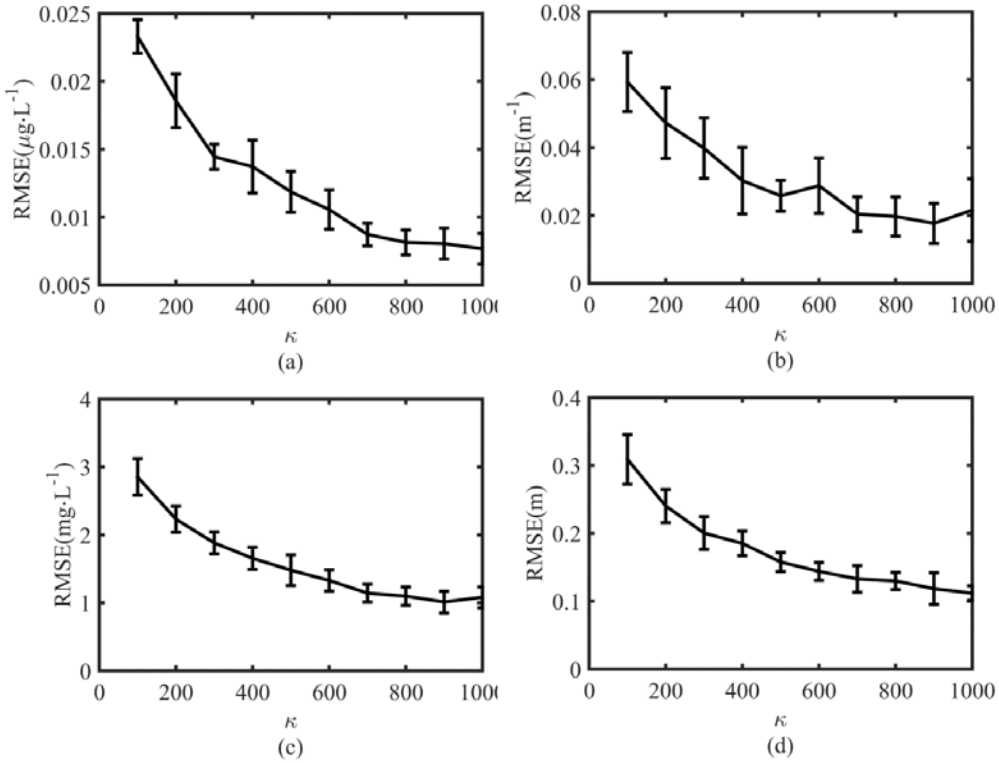

Training sample size is determined as 1000 according to the sensitivity analysis. Each experiment will be repeated for 40 times, the mean and the standard deviation values are reported

Data fusion, constraint with LiDAR

Semianalytical Model: $R(\lambda) = f(C_{CHL}, C_{CDOM}, C_{NAP}, d)$

The water depth d can be input from LiDAR bathymetry.

nLSQ: the LiDAR depths are used to constrain the solution and reduce the number of parameter from 4 to 3;

mSVR: the LiDAR depth map is concatenated in the hyperspectral imagery as the extra feature.

nLSQ, unconstrained

(a) is the CHL concentration map,
(b) is the measure of CDOM,
(c) is the NAP concentration map,
(d) is the water bathymetry

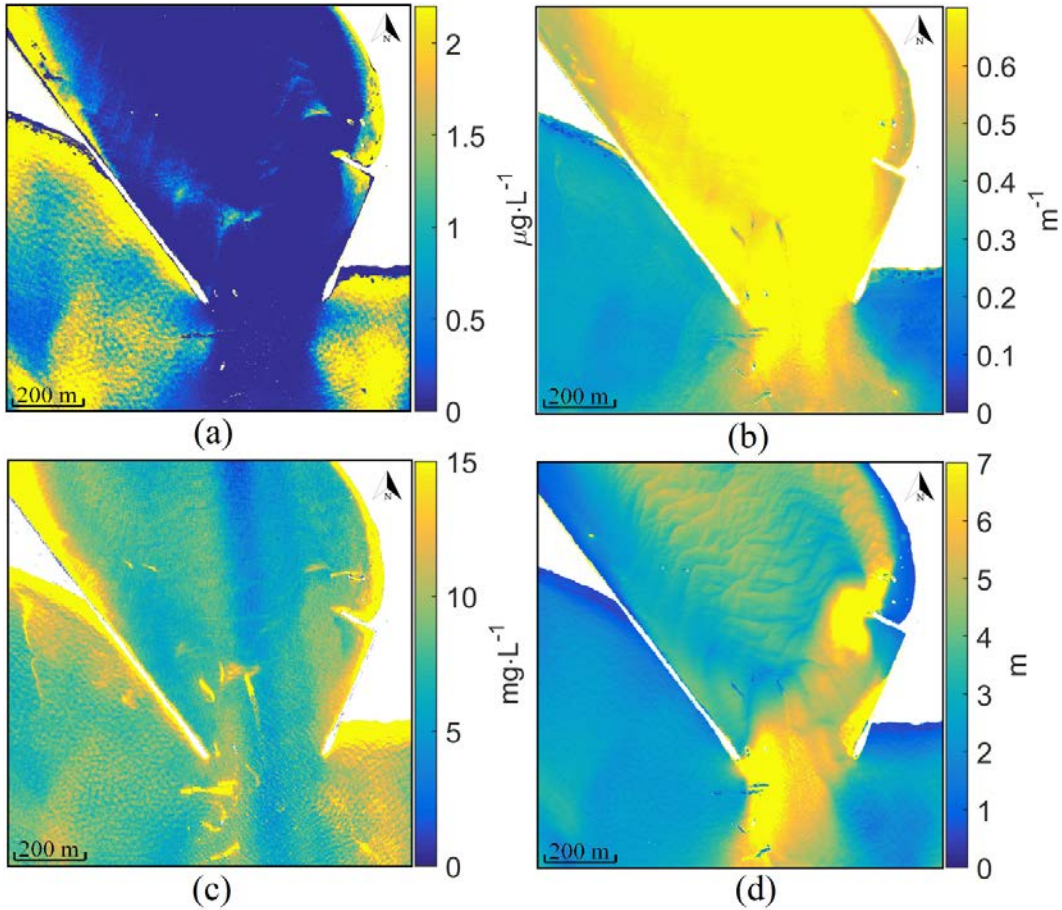

nLSQ, constrained

(a) is the CHL concentration map,
(b) is the measure of CDOM,
(c) is the NAP concentration map,
(d) is the water bathymetry

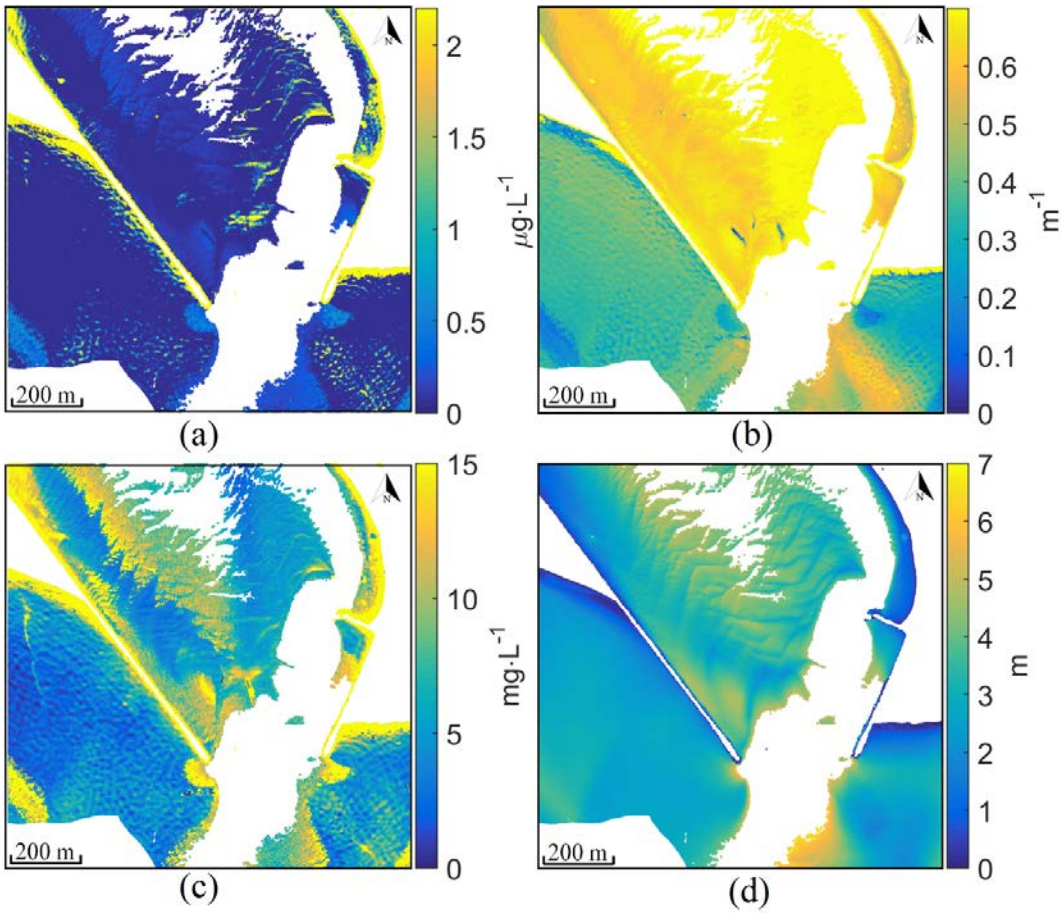

mSVR, unconstrained

(a) is the CHL concentration map,
(b) is the measure of CDOM,
(c) is the NAP concentration map,
(d) is the water bathymetry

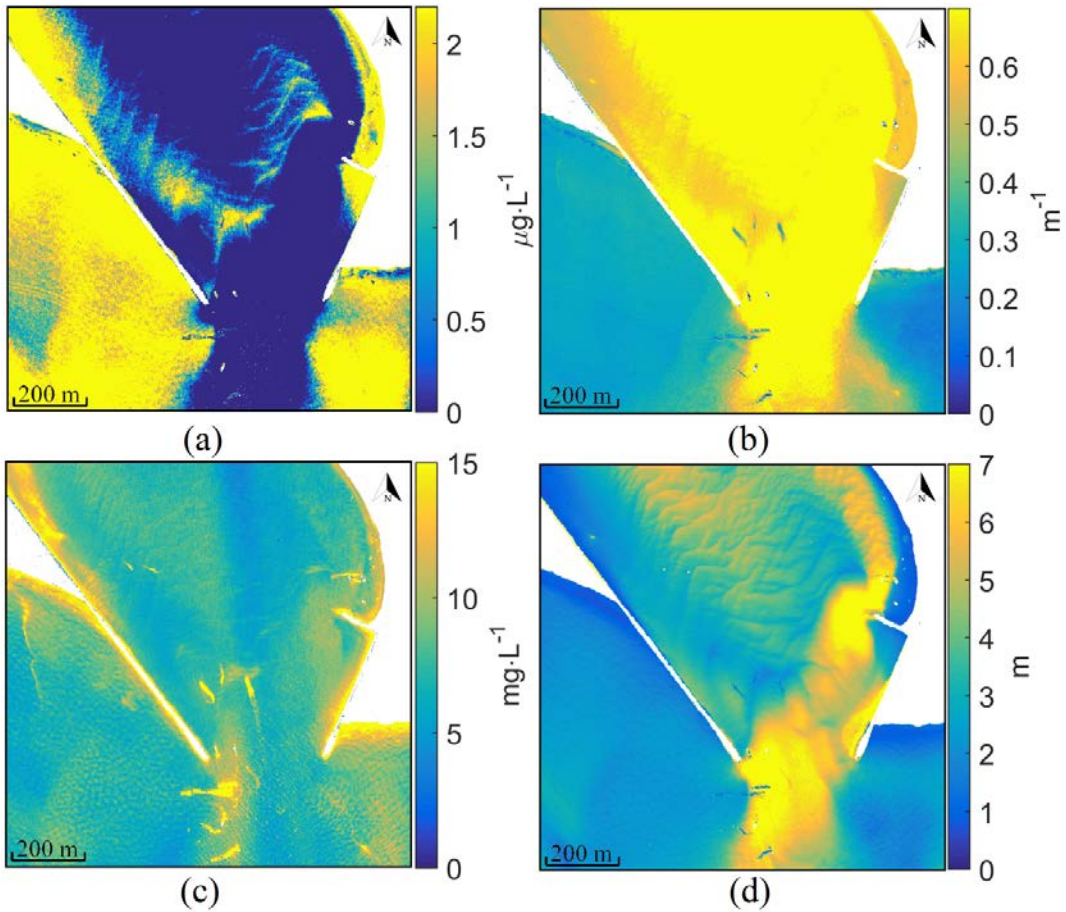

mSVR, “constrained”

(a) is the CHL concentration map,
(b) is the measure of CDOM,
(c) is the NAP concentration map,
(d) is the water bathymetry

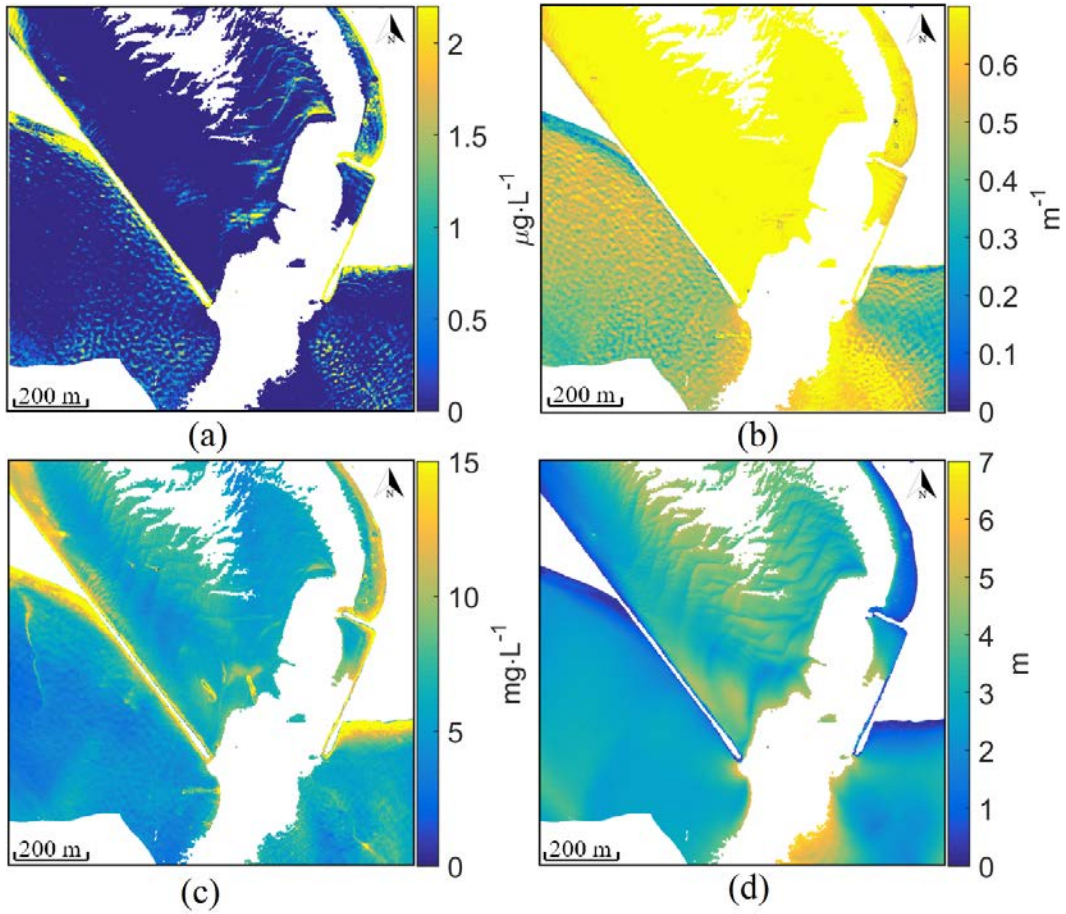

Comparison-Four bathymetry products

- **ASVR**

  The bathymetry product estimated with SVR method and ADCP field measured water depth samples (423 samples)

- **LSVR**

  The bathymetry product estimated with SVR method and LiDAR measured water depths (1000 samples)

- **nLSQ**

  The bathymetry product estimated with the nLSQ unconstrained method

- **mSVR**

  The bathymetry product estimated with the mSVR unconstrained method (1000 samples)

Bathymetry products comparison

(a) ASVR bathymetry map,
(b) LSVR bathymetry map,
(c) nLSQ bathymetry map,
(d) mSVR bathymetry map.

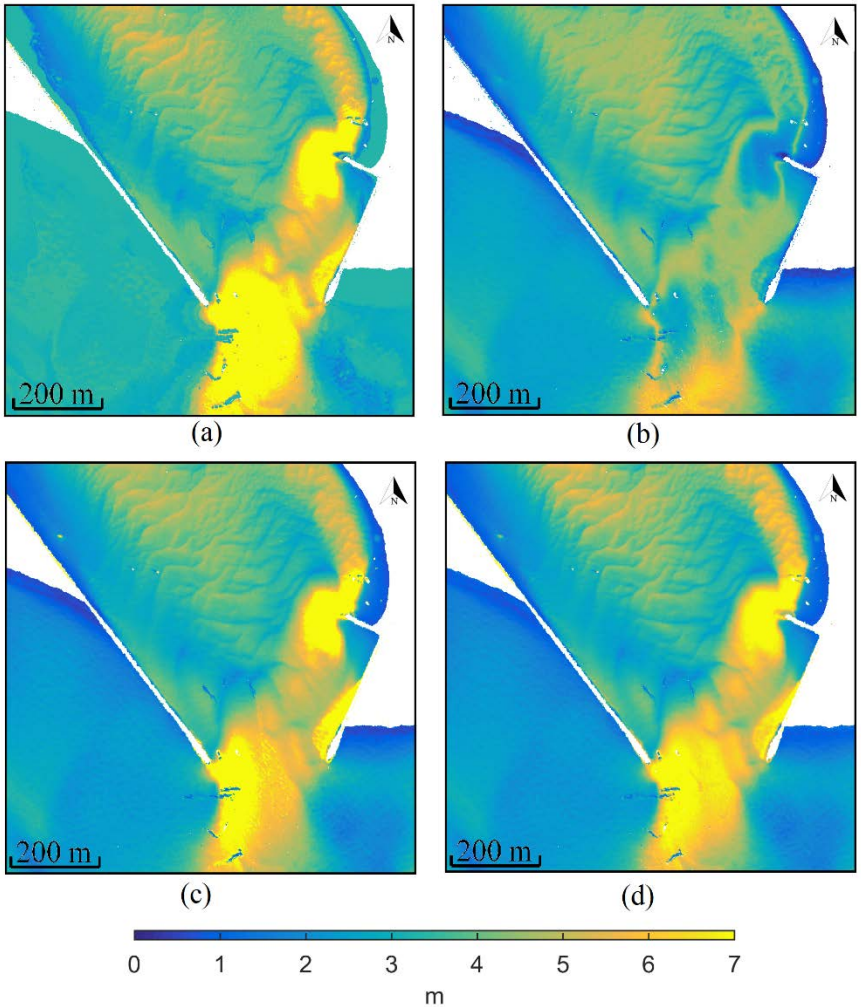

Comparison

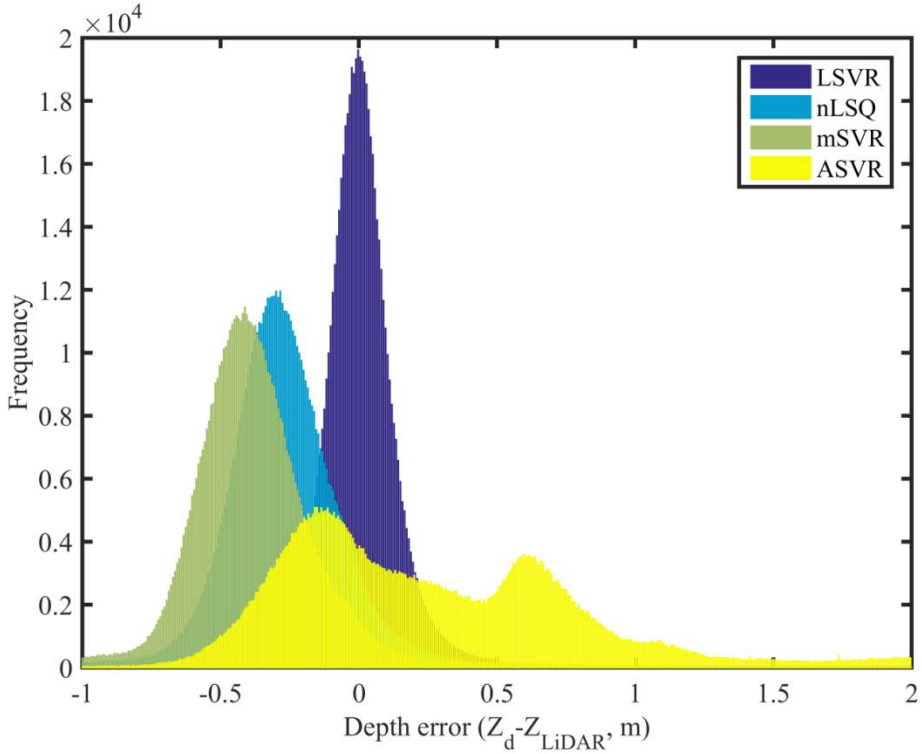

- LSVR yielded the best accuracy;
- ASVR yielded the least accuracy;
- nLSQ and mSVR both show offsets to the LiDAR depths;
- nLSQ and mSVR both show moderate accuracy.

	ASVR	LSVR	nLSQ	mSVR
Mean (m)	0.25	0.01	-0.28	-0.40
Standard deviation (m)	0.51	0.13	019	0.20
RMSE (m)	0.57	0.13	0.34	0.44
Median (m)	0.15	0.00	-0.29	-0.41
IQR (m)	0.75	0.14	0.22	0.23

Bathymetry products comparison

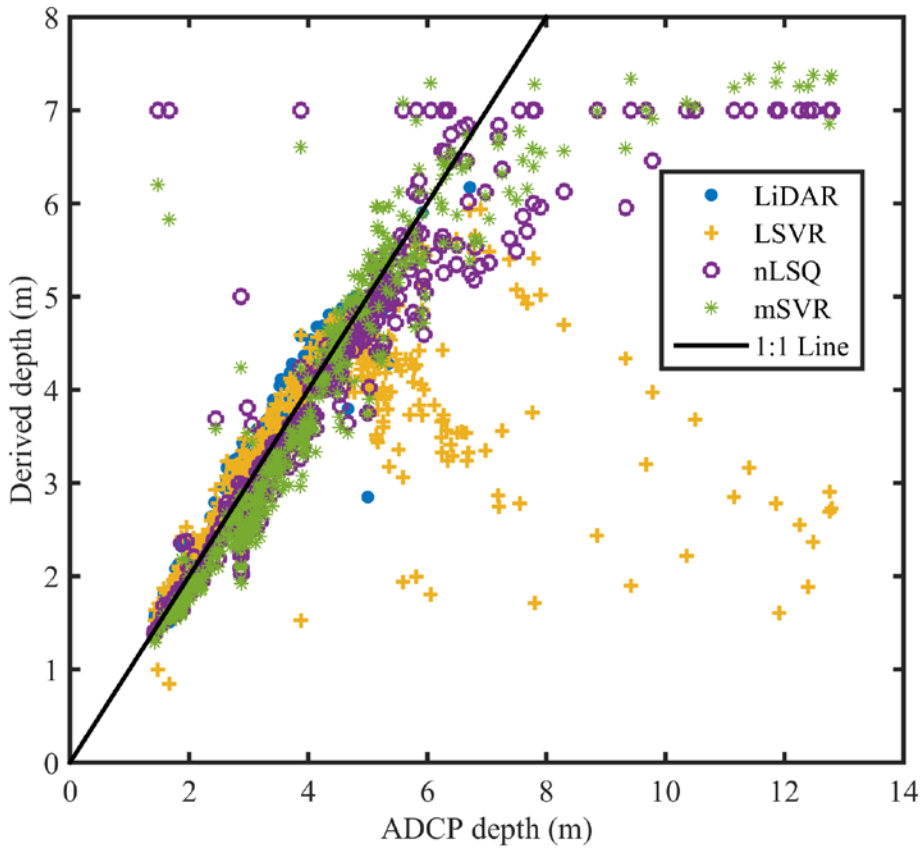

LSVR deviates after 5 meters due to less samples available in this range, mSVR and nLSQ deviate after 6 meters due to the insignificant benthic reflectance.

Discussion

Several potential improvements for a further study:

1. Alternative chlorophyll spectra models or field measured chlorophyll spectra;
2. Experiments with varying benthic types site, regularizing techniques applied in the semianalytical model;
3. Hyperspectral imagery has better performance than the fusion in this study, but the fusion needs more investigations;
4. Better LiDAR bathymetry product with deeper penetration is desired to fully assess the benefits of fusing LiDAR and hyperspectral imagery;

Thanks